An Article Submitted to

INTERNATIONAL JOURNAL OF CHEMICAL REACTOR ENGINEERING

Residence Time Distribution Determination of a Continuous Stirred Tank Reactor using Computational Fluid Dynamics and its Application on the Mathematical Modeling of Styrene Polymerization

Ignacio L. Gamba[*] Santiago Marquez Damian[†] Diana A. Estenoz[‡]
Norberto Nigro[**] Mario A. Storti[††] David Knoeppel[‡‡]

[*]Instituto de Desarrollo Tecnológico para la Industria Química INTEC (CONICET-UNL) Argentina, igamba@intec.unl.edu.ar

[†]Instituto de Desarrollo Tecnológico para la Industria Química INTEC (CONICET-UNL) Argentina, santiagomarquezd@gmail.com

[‡]Instituto de Desarrollo Tecnológico para la Industria Química INTEC (CONICET-UNL) Argentina, destenoz@santafe-conicet.gov.ar

[**]Instituto de Desarrollo Tecnológico para la Industria Química INTEC (CONICET-UNL) Argentina, nnigro@santafe-conicet.gov.ar

[††]Instituto de Desarrollo Tecnológico para la Industria Química INTEC (CONICET-UNL) Argentina, mstorti@intec.unl.edu.ar

[‡‡]TOTAL Petrochemicals USA, david.knoeppel@total.com

ISSN 1542-6580

Residence Time Distribution Determination of a Continuous Stirred Tank Reactor using Computational Fluid Dynamics and its Application on the Mathematical Modeling of Styrene Polymerization*

Ignacio L. Gamba, Santiago Marquez Damian, Diana A. Estenoz, Norberto Nigro, Mario A. Storti, and David Knoeppel

Abstract

The continuous operation of a stirred tank reactor for styrene polymerization was modeled. The proposed approach consists of an iterative procedure between two modules that considers the fluid-dynamics and kinetics respectively. The kinetic module considers a complex kinetic mechanism and is used to predict the time evolution of global variables, such as conversion and species concentrations, physicochemical properties and molecular structure characteristics of the final product. In order to obtain a 3D representation of the flow field, the simulation of the hydrodynamics of the reactor was carried out with the aid of a commercial computational fluid dynamics (CFD) software package. Because CFD is capable to predict the complete velocity distribution in a tank, it provided a good alternative to carry out residence time distribution (RTD) studies. It was found that the stimulus-response tracer method is reasonably accurate to obtain a complete RTD compared to the particle tracking method. The obtained RTD results showed a good agreement when validated with experimental data and literature information.

From the estimates of the kinetic module and the RTD predictions, a statistical calculus allows the determination of the average properties at the reactor outlet. The convergence of the iterative procedure was tested and reasonable predictions were achieved for an industrial reactor.

KEYWORDS: CFD, residence time distribution, CSTR, polymerization

---

*The authors would like to acknowledge: CONICET, Universidad Nacional del Litoral, Total Petrochemicals USA, and ANPCyT for providing financial support for this research.

1. INTRODUCTION

Polymer industry has been undergoing a major change in various standards over the past few decades. Current efforts are more focused on product quality and performance, along with better productivity. Mixing is an important operation in chemical engineering and deserves particular attention in a polymerization process because polymeric materials must be produced with required specifications (Brooks, 1997). The quality of a polymer formed by polymerization is strongly affected by the nature of mixing and, hence, a better understanding of the impact of mixing is necessary. Continuous stirred-tank reactors (CSTR) are still widely used in polymerization processes. Short-circuiting, dead zones, and recirculation are some of the key mixing parameters defining the degree of mixing in a CSTR (Saeed et al., 2008a; 2008b). In fact, the degree of mixing significantly affects the reagents conversion, as well as the molecular structure of the final product.

In previous works, several researchers (Harada, 1968; Cole, 1975; Prochukhan et al., 1988; Tosun, 1992; Kemmere et al., 2001; Heidarian et al., 2004; Dhib et al., 2010; Ein-Mozaffari et al., 2010) have asserted a strong relationship between the polymerization rate, the final polymer properties, and the nature of mixing in a polymerization process. Harada et al. (1968) discussed the effect of micro-mixing on the homogeneous polymerization of styrene (St) in a continuous flow reactor. Cole (1975) carried out an experimental study of mixing patterns in CSTRs for anionic solution polymerizations of butadiene and their effect on polymer structure. Prochukhan et al. (1988) studied the use of different agitation methods in a polymerization of isobutylene. Kemmere et al. (2001) described the influence of the characteristics of emulsification on the course and outcome of a batch-emulsion polymerization of St and vinyl acetate. Heidarian et al. (2004) studied the impact of the temperature and mixing rate in a polymerization reaction to produce fatty polyamides in the presence of catalyst. Dhib et al. (2010) and Ein-Mozaffari et al. (2010) discussed the effects of the impeller speed and the residence time on the conversion and flow behavior in a laboratory-scale CSTR for St polymerization.

The quantified residence time distribution (RTD) provides an approach to characterize the non-ideal mixing in a reactor, thus allowing the process engineer to better understand mixing performance of the reactor (Levenspiel, 1999; Hayes, 2001). The RTD information can be used to design an appropriate reactor model system to reflect the actual mixing behavior in the tank. An appropriate reactor model, when furnished with accurate reaction kinetics, can provide accurate predictions of reactor performance and aid in both process design and optimization (Levenspiel, 1999; Hayes, 2001; Ranade, 2002). Numerous experimental studies on RTD in continuous stirred tanks have been carried out

over the years, covering a wide range of tank sizes, impeller designs, baffle designs and operating conditions (feed flow rates and impeller rotation rpms) (Zaloudik, 1969; Levenspiel et al., 1970; Turner, 1971; Li and Lee, 1991; Newell et al., 1998).

Viscosity changes rapidly during polymerization, and in general a non-ideal CSTR behavior is observed. Therefore, a model capable of incorporating the non-ideal flow behavior is needed. Recent advancements in numerical modeling techniques have made possible to adopt the computational fluid dynamics (CFD) approach to build such non-ideal models for polymerization reactors, providing a more detailed insight into the complex hydrodynamics and mixing processes. Recent advances in the study of mixing phenomena using CFD have been developed (Harshe et al., 2004; Yiannoulakis et al., 2001; Hatzantonis et al., 2000). However, the use of CFD has not been completely exploited in polymerization processes and relatively few studies have been published (Mahling et al., 2000; Tosun et al., 1997; Read et al., 1997; Bakker et al., 2001; Wells and Ray, 2001; Kolhapure and Fox, 1999; Zhou et al., 2001; Soliman et al., 1994; Meszena et al., 2001; Dhib et al., 2010, Ein-Mozaffari et al., 2010).

Mahling et al. (2000) used CFD to investigate a high-pressure low density polyethylene (LDPE) tubular reactor. Since the polymerization kinetics was not considered, the effect of viscosity on the reactants mixing was not completely evaluated. Similarly, Tosun and Bakker (1997), Read et al. (1997), Bakker et al. (2001), and Wells and Ray (2001) used the CFD approach to investigate a LDPE polymerization reactor. Kolhapure and Fox (1999) utilized CFD to simulate ethylene polymerization in a tubular reactor and observed a reduction of ethylene conversion and an increase of the polydispersity index due to an imperfect mixing. Zhou et al. (2001) employed CFD to predict the initiator consumption and the molecular weight distribution of the LDPE. Soliman et al. (1994) and Meszena et al. (2001) used CFD to simulate polystyrene (PS) radical and living polymerization in tubular reactors respectively. Due to the plug flow characteristics, the convergence of the CFD simulation was easily achieved. Ein-Mozaffari et al. (2010) adopted the CFD approach to simulate benzoyl peroxide (BPO)-initiated St polymerization with a simplified kinetic mechanism in a simple laboratory-scale CSTR and investigated the effects of the impeller speed and the residence time on the conversion and the flow behavior.

Because CFD is capable of predicting the complete velocity distribution in a vessel, it provides an alternative and simpler mean of determining the RTD. With the rapid advance of computational technology, increasing numbers of studies on RTD in reactors and mixers using CFD have been published in recent years (Ranade, 2002; Ghirelli et al., 2006; Vedantam and Joshi, 2006; Atiemo-Obeng et al., 2004; Ring et al., 2004) including a limited number of publications on RTD in continuous stirred tanks (Ring et al., 2004). Ring made RTD

measurements for both a baffled and an unbaffled laboratory reactor with a Rushton turbine operating with water at different feed flow rates and impeller rpms. The experimental results were compared to CFD predictions of the RTD obtained by the stimulus-response tracer method.

Few studies related to CFD applied to PS process have been published (Dhib et al., 2010; Ein-Mozaffari et al., 2010). In this work, a new approach to simulate the continuous operation of a stirred tank reactor for St polymerization is presented. A RTD study based on two different CFD methods is carried out and the results are coupled with a detailed mathematical St polymerization model. CFD results were validated with different experimental data and very good agreements were obtained in all cases. The aim of simulating a CSTR for St polymerization is to evaluate the effect of the fluid-dynamics (FD) and kinetics on the performance of the reactor, obtaining not only global variables, such as conversion and species concentrations, but molecular structure characteristics of the final product. The importance of this study lies in the interaction between the kinetic and FD phenomena that will lead us to solve a challenging problem of polymerization reaction engineering: obtain recipes and reaction conditions (reagents concentrations, temperature, initiator types, stirring system, reactor type, etc.) for the production of a priori specified grades of PS.

2. MODELING OF THE FLUID-DYNAMICS OF A CSTR

In order to model the FD of a CSTR and to determine detailed information on fluid flow, the CFD commercial package Fluent 6.3 was used. The model is presented in Appendix A and is basically constituted by the continuity and momentum balance equations that are solved using CFD assuming steady-state conditions.

2.1 Flow field simulation. General considerations

To solve the differential equations numerically, the system is discretized through a grid. To this effect, the domain of integration (volume occupied by the fluid) is divided into a set of discrete sub-domains, or computational cells. Fine mesh resolution is used for the regions with potentially high velocity gradients, such as the regions at the impeller tips. The resolution of the computational grid is a key factor in any CFD simulation as this is directly related to the computational cost of the solution.

In order to solve equations A.1-A.9 numerically, CFD commercial package Fluent utilizes the Finite Volume Method. The result of the discretization process is a finite set of coupled algebraic equations that need to be solved simultaneously in every cell of the solution domain. The Second Order Upwind

discretization scheme was chosen for all equations in order to minimize numerical diffusions. An Upwind scheme was used for reasons of numerical stability of the spatial advection operator. Upwind normally results in the addition of numerical diffusion to stabilize the numerical scheme and, in order to prevent contamination of the solution with this extra diffusion, "High Resolution Schemes" were used in Fluent through a second order upwind discretization scheme. In addition, standard scheme was used for the pressure discretization and the pressure-velocity coupling was solved using SIMPLE algorithm.

The impeller motion was modeled using the multiple reference frames (MRF) method. A weak interaction between the rotating impeller blades and the stationary tank wall and baffles was assumed. The reactor tank was divided into two regions: an inner region attached to the rotating impeller and shaft; and an outer region attached to the stationary baffles and the vessel. The momentum equations for the inner region are solved using a rotating framework, whereas the equations for the outer region are solved using a stationary framework. The solution is matched at the interface of the rotating and stationary regions via a velocity transformation from one frame to the other. This velocity-matching step implicitly involves the assumption of steady flow conditions at the interface.

An inlet-velocity boundary condition at the feed stream and a pressure outlet boundary condition to the tank output were considered. For the walls of the tank, baffles, and the other tank internals, Standard Wall Function boundary conditions were assigned. These are special boundary conditions that are normally used in turbulent flows and that depend on the flow conditions prevailing in the area near the boundary. Finally, a traction force is determined as a function of the friction speed at the wall instead of imposing the velocity on the wall itself.
An interface boundary condition to the surface of the moving zone, and a (stationary) standard wall function inside the rotating mesh to the surface of the impeller were assigned. The model was allowed to run using double precision calculations until all the scaled residuals reached a value of 10^{-5}.

2.2 RTD calculation with CFD

Two methods were studied in order to predict the RTD from the flow field: the Particle Tracking method and the Stimulus-Response Tracer method. Both of them take a two-step approach in which the first step is to solve the flow field. This flow field remains fixed for the subsequent step in both methods. The methods differ in their second step.

2.2.1 Particle Tracking Method

The trajectory of a discrete phase particle can be predicted with Fluent by integrating the following force balance on the particle in a Lagrangian reference frame:

$$\frac{du_p}{dt} = F_D \cdot \left(u - u_p\right) + \frac{g_i \cdot \left(\rho_p - \rho\right)}{\rho_p} + F_i' \tag{1}$$

To consider massless particles, Fluent's particle tracking model was adapted using infinitesimal particles that follow the velocity field except in a relaxation time τ. The trajectories of the infinitesimal particles are solution of the well-known differential equation:

$$\frac{dx_i}{dt} = u_i \tag{2}$$

This method is probabilistic (based on Montecarlo-like method), since particles are injected at random points at the inlet. Its advantage is that the computation for each particle is completely independent of the other.

When dealing with turbulent flows, the momentum equation for the particle has a drag force term related to a stochastic process, resulting in a stochastic differential equation (SDE).

To apply the particle tracking method, an axial CSTR agitated by two stages of two-bladed type impeller was simulated. Water at 25ºC (density = 998 kg/m^3, dynamic viscosity = 9.10^{-4} kg/ms) was considered as the test fluid. Assuming constant physicochemical properties, the reactor RTD was obtained from stochastic particle tracking, which tracks residence times of massless tracers through the tank. In this method, once the fixed flow field is solved, massless tracers are released at the inlet, and the particle trajectories are calculated using a Lagrangian method. The tracers are defined as very small particles (1 μm diameter) with the same density as the liquid and, therefore, follow the flow pattern. The dispersion of tracers due to turbulent eddies was calculated with the Random Walk model, which provides a random perturbation over the local mean flow.

Since the process is probabilistic, a sufficient number of particles (10,000) were tracked to balance the random effects of turbulent eddies and produce statistically significant results (Ghirelli et al., 2006). In the simulations, the time step is controlled by the number of steps required for a particle to pass the smallest computational cell. A number of 20 was found to be adequate and was

used for the modeling of the reactor (Ring et al., 2004). The recorded residence times for all tracers were then combined to obtain the RTD, and the mean residence time was calculated.

The resultant RTD was verified by comparing the mean residence time with the tank space time, which is simply the liquid volume in the tank divided by the volumetric flow rate. A low performance of this method was obtained when comparing the resulting mean RT (t_m=30 min) with the tank space time ($V_R/Q \approx$ 15 min), showing a significant discrepancy.

When the dispersed phase model is combined with the MRF model, the particle motion in the rotating frame should be incorporated as well. While there are techniques available to that effect, it is not clear whether the results are meaningful in all reference frames. It was reported that this combination of models should therefore be avoided (Handbook of Industrial Mixing. *Wiley*, 2004).

There are three types of errors while calculating the trajectories of particles in a discrete phase modeling: discretization, time integration, and round-off. In regular laminar flows the error in the particle location increases as t^2, and in turbulent flows it increases almost exponentially.

As it was reported, this method is not recommended because it is not possible to avoid particles trapping in recirculation regions even for laminar flows and the resulting integral distribution function E(t) is considerably distorted, especially for long times (Thyn et al., 1998). In addition, there are almost no publications reporting the numerical treatment of RTD using particle tracking, which seems to be an open question. There are not a sufficient number of studies to conclude anything about the utility of this tool or about the error inherent to this technique.

2.2.2 Stimulus-Response Tracer Method

This method basically mimics the methods used in experimental measurements of RTD. In this method, a non-reactive tracer is introduced into the system at the inlet. The concentration of the tracer is changed according to a known function and the response is found by calculating the concentration of the tracer at the outlet. It is assumed that the selected tracer does not modify the physical characteristics of the fluid and its introduction does not affect the hydrodynamic conditions.

The determination of the response to an input step can be determined numerically by solving the advection diffusion equation. In contrast to the method of particle tracking, this method is deterministic since the result is not depending on the generation of a random sequence.

The stimulus-response tracer method was tested and simulated with the same reactor used with the particle tracking method. The former showed a good performance and it was reasonably accurate to obtain a complete RTD.

2.3 RTD Determination

2.3.1 Geometry

In order to validate experimentally the RTD results obtained with the stimulus-response tracer method, the geometry of a 1275 ml laboratory continuous stirred tank was modeled. The geometry of the CFD model is shown in Figure 1 and all internal dimensions are indicated in Table 1. The stirring system is a standard two-bladed impeller without baffles. There is an internal pipe protruding into the reactor from its top, which is the feed tube that ends at the approximate height of the impeller. There is also an outlet tube at the top of the tank.

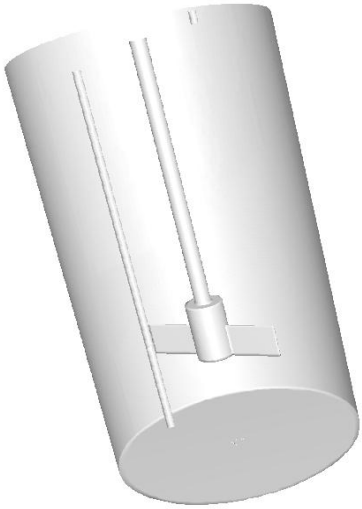

Figure 1**.** Laboratory reactor geometry

The three dimensional geometry was built with the aid of the commercial grid generator package Gambit (Fluent Inc.). The total grid has 1 million cells approximately. The volume mesh was created using a Cooper scheme, where a 'source' surface is meshed with quadrilaterals and these quadrilaterals are then extruded through the volume towards a 'target' surface generating layers of hexahedra along the way. This results in a structured grid of hexahedral volume elements. To ensure a good quality mesh, attention was paid to neither exceed 0.85 for the EquiAngle skewness nor 1.2 for the size ratio between adjacent cells.

Table 1. Dimensions of the laboratory continuous stirred tank

	Description	Dimension (mm)
Tank	Diameter	95
	Height	180
Impeller	Blade height	13
	Blade width	20
	Blade thickness	1.5
	Diameter	54
Inlet tube	Inside diameter	4
	Outside diameter	6
	Radial position of centerline	40
Outlet tube	Inside diameter	4
	Outside diameter	6
	Radial position of centerline	40

2.3.2 Flow field in the reactor

The generated grid was loaded into Fluent 6.3 for resolution of the flow field. The operating conditions for this study consisted of a flow rate of Q = 430 ml/min and a stirring rate of N = 100 rpm. Water was used also as the test fluid. Based on the value of the Reynolds number at the tip of the blades (Re=5000), the flow falls into a transition regime around the impeller. A low Reynolds k-ε model was used as the turbulent model. Figure 2 shows the predicted velocity magnitude contours.

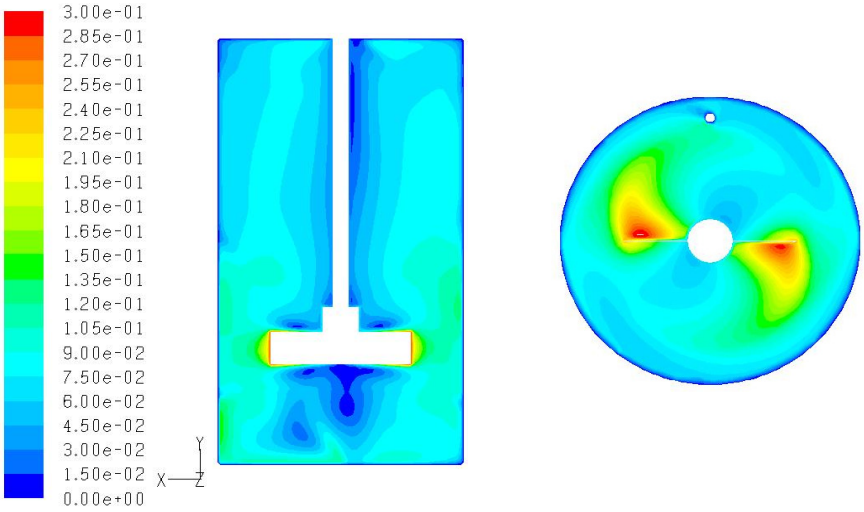

Figure 2. Contours of velocity magnitude obtained from laboratory reactor

The consistency in terms of velocity was verified by checking that the tangential magnitude at the impeller tips is in agreement with the applied stirring rate N. The model was allowed to run using double precision calculations until all the scaled residuals had reached a value of 10^{-5}.

2.3.3 RTD Prediction

The behavior of the tracer was modeled by fixing the fluid flow field and by adding a user defined scalar to model the concentration of a tracer with a zero diffusion coefficient. The boundary conditions for the tracer consisted of a feed mass fraction equal to 1.0. The simulation was allowed to proceed using time steps of 1 s.

A transient simulation of passive scalars was created and the outlet response to a step input at the inlet was predicted. In a step experiment, the tracer concentration at the reactor inlet changes abruptly from 0 to C_0. The tracer concentration at the outlet was collected from the simulation, normalized to the concentration C_0 and plotted against time, obtaining the non-dimensional curve F(t) of Figure 3.a:

$$F(t) = \frac{C(t)}{C_0} \tag{3}$$

By differentiating the curve of Figure 3.a, the RTD of Figure 3.b was estimated according to:

$$F(t) = \int_0^t E(t)dt \longrightarrow E(t) = \frac{dF(t)}{dt} \tag{4}$$

The mean RT (t_m) is calculated by integrating the RTD as follows:

$$t_m = \int_0^\infty tE(t)dt \tag{5}$$

The resultant mean RT predicted with Fluent (t_m=172 s) was in good agreement with the tank space-time (V_R/Q=177 s).

The variance or square of the standard deviation of the RTD was calculated from:

$$\sigma^2 = \int_0^\infty (t - t_m)^2 E(t)dt \tag{6}$$

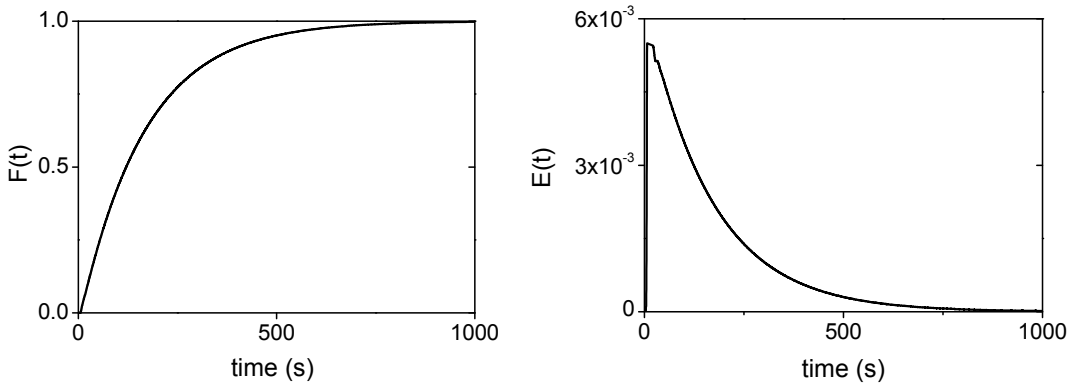

(a) (b)

Figure 3. Laboratory reactor simulation: (a) step response; (b) RTD

The magnitude of this 2nd moment is an indication of the spread of the RTD. For this simulation a value of σ/t_m=0.95 was obtained, which is similar to the one of an ideal reactor.

In the attempt of using a pulse input method in the simulations, it was found that the concentrations were very small and round off errors were sufficiently large as to invalidate the overall mass balance significantly beyond the convergence criterion, therefore invalidating RTD predictions. For this reason, the step method for determining the RTD was used in all the simulations.

3. CFD MODEL VALIDATION

3.1 Experimental work

In order to validate RTD results for a CSTR obtained with CFD, an experimental work was carried out. The experimental system is shown in Figure 4. The output stream flows directly into a conductimeter flow cell that is connected to a data acquisition system collecting data at time intervals of 1 s.

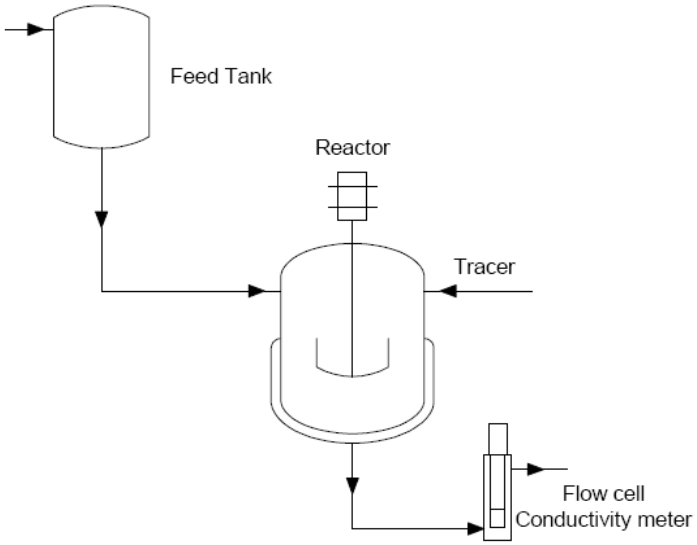

Figure 4. Experimental equipment

A volume of 1 ml of an inert chemical tracer (a concentrated solution of 200 g/L NaCl in water) was injected into the tank at time zero. Water at 25°C was used as the test fluid. The on-line conductimeter allows the detection of the salt concentration C(t), by measuring the conductivity of the outlet stream. The experimental conditions used to measure RTDs are given in Table 2. For all experiments, data were taken at 1 s intervals. The experiments were done by duplicate or triplicate in order to check the repeatability of the measurements.

As it can be observed in Table 2, the mean RT decreases with increasing stirring rate until a constant value is reached. This constant value is approximately V_R/Q, the space-time for the tank.

The collected conductivity data from the experiments is plotted in Figure 5 at different impeller rates. All of these curves show a fast increase at an early time followed by an exponential decrease as expected for an ideal CSTR. In addition, although great care was taken in synchronizing the pulse input with the initiation of data accumulation, the computer program shows an initial delay of the data acquisition.

Table 2. Experimental conditions and results for RTD measurements

Flow rate Q (ml/min)	Impeller speed (rpm)	Mean residence time t_m (s)	σ/t_m	Tank space-time V_R/Q (s)
430	0	193	0.79	177
	50	190	0.80	
	100	186	0.82	
	200	185	0.91	

The RTD is obtained from the experimental data by normalization as follows:

$$E(t) = \frac{C(t) - C(t=0)}{\int_0^\infty [C(t) - C(t=0)]dt} \tag{7}$$

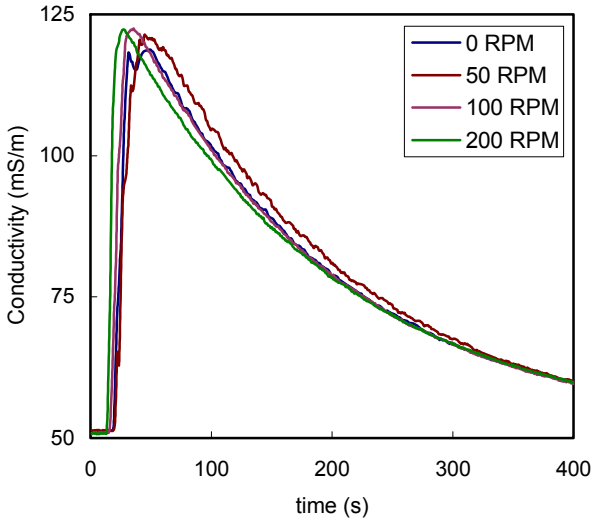

Figure 5. Laboratory reactor experiment: Concentration profile measured through the conductivity

In Figure 6, the measured RTD (at 100 rpm) is plotted together with the ideal RTD and the RTD predicted by Fluent. The mean RT (t_m) was calculated by integrating the RTD. The variance or square of the standard deviation of the RTD was also estimated (see Table 2). At higher impeller rates, the value of σ/t_m is close to 1 as expected for ideal stirred tanks.

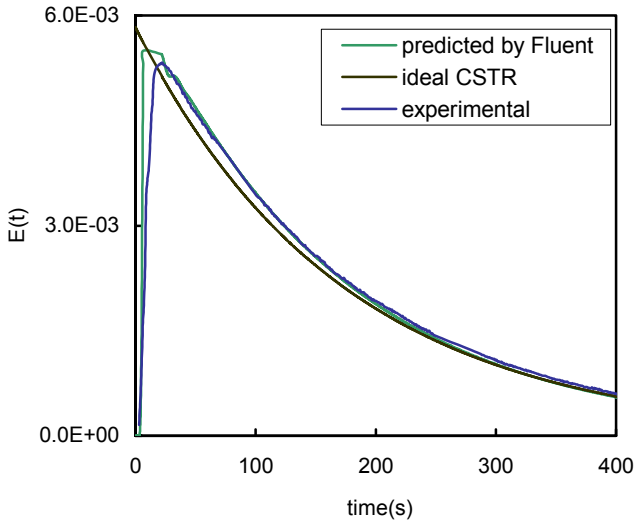

Figure 6. Comparison of experimental result of RTD, CFD prediction, and calculated ideal $E(t)$ for a perfectly mixed CSTR.

Even for the good mixing case shown in Figure 6, there are deviations from ideal mixing at short residence times where the initial rise is not immediate and does not lead to a smooth curve. For comparison purposes, this figure contains a plot of the ideal RTD for a CSTR. Experimental results show a significant agreement with theoretical predictions for an ideal CSTR.

Figure 6 also shows a comparison of the Fluent-predicted RTD and the experimentally measured RTD. A good agreement between experimental and CFD-predicted RTD is observed. Table 3 summarizes the results obtained from the CFD model and the experimental work.

Comparing the experimentally measured and CFD predicted RT values with the expected theoretical value V_R/Q, a discrepancy less than 5 % was observed.

Table 3. Experimental and predicted RTD results

Flow rate Q (ml/min)	Space-time V_R/Q (s)	RPM	Experimental		CFD	
			t_m (s)	σ/t_m	t_m (s)	σ/t_m
430	177	100	186	0.82	172	0.95

3.2 Other validation of CFD prediction

To further investigate the reliability of Fluent as a prediction tool, a CSTR geometry taken from literature (Ring et al., 2004) was modeled. In this study, CFD results are compared with the reported experimental data.

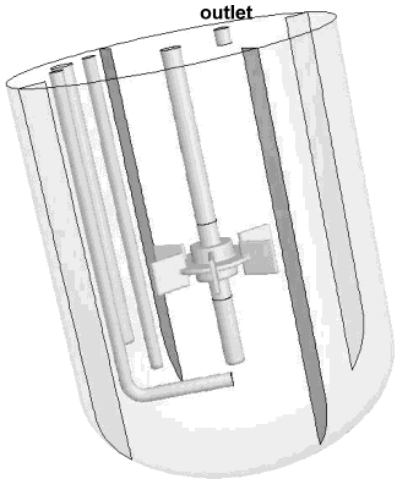

Figure 7. Reactor geometry (taken from Ring et al. (2004))

The geometry of the 1400 ml laboratory baffled stirred tank reactor is shown in Figure 7. The baffled reactor has four equally spaced baffles at 90º and is agitated by a standard six-bladed Rushton turbine impeller. Regarding to the grid resolution in the present CFD model, a hexahedron-dominant mesh was used for the tank domain in order to achieve an efficient mesh resolution. The total number of cells was approximately 6.10^5.

The stimulus-response tracer method was used to predict the RTD of the stirred tank. The first step was to solve the flow field of the tank. Water was used as the test fluid. With a Reynolds number of approximately 3000 at the tips of the blades, a transition flow regime was found around the impeller. The low Reynolds k-ε model was used as the turbulent model, obtaining a good convergence. Figure 8 shows the velocity magnitude contours of the stirred tank reactor. The observed velocity discontinuity is due to the cut plane through the baffles.

As it was previously explained, after the resolution of the fixed flow field, a user defined scalar was added to model the concentration of the tracer and the outlet response to a step input was predicted. The evolution of the tracer concentration is shown in Figure 9.a. The model was allowed to run until all the scaled residuals reached a value of 10^{-5}. From the concentration data obtained at the outlet, the RTD of the tank was obtained and it is represented in Figure 9.b.

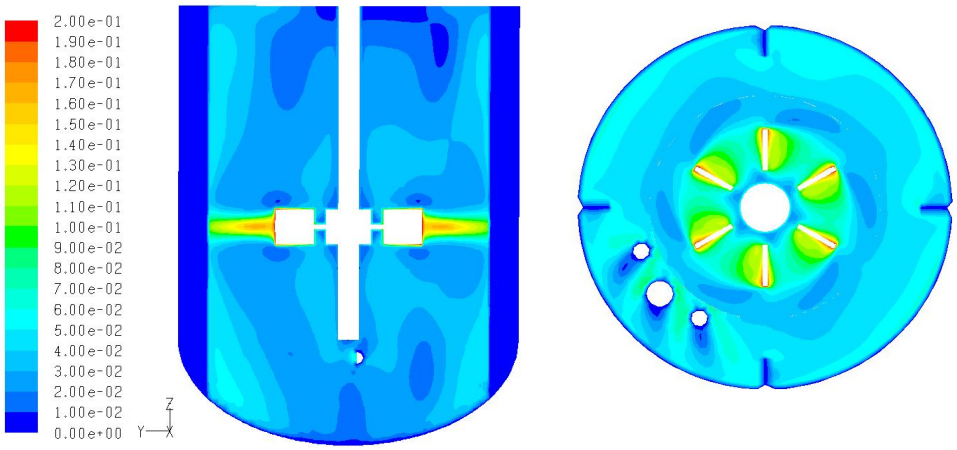

Figure 8. Contours of velocity magnitude (for reactor of Ring et al. (2004))

Table 4 summarizes the experimental conditions and results from Ring et al. (2004) and the results obtained from the CFD model. A good agreement was obtained.

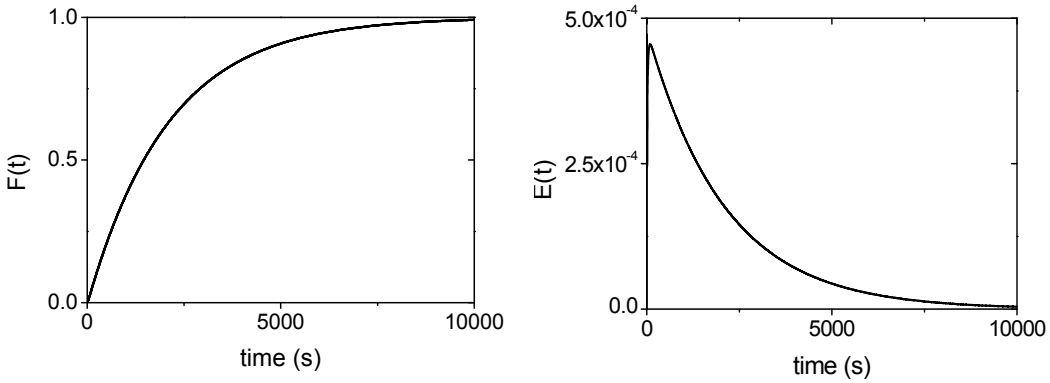

(a) (b)

Figure 9. For reactor of Ring et al. (2004): (a) step response; (b) RTD

Table 4. Experimental data from Ring et al. and predicted RTD results

Flow rate Q (ml/min)	Space-time V_R/Q (min)	RPM	Experimental (Ring et al., 2004)		CFD	
			t_m (min)	σ/t_m	t_m (min)	σ/t_m
40	35	80	35.4	0.99	35	0.99

The previous CFD studies make a contribution to validate and provide the expected RTD for a laboratory CSTR with water as the test fluid. However, the experimental conditions presented differ from what actually occurs in a PS CSTR. First of all, the viscosities exhibited by water are far from the viscosities at 30% conversion present in a real PS industrial reactor. This difference in viscosities may have an effect on the RTD. Additionally, it is well known that real PS CSTRs use either anchor or helical ribbon impellers in order to handle the high viscosities present in these systems.

To this effect, a 3D geometry of a real PS reactor was built according to industrial drawings. Due to confidentiality reasons, the geometry can not be displayed in this work.

In order to validate the industrial CFD model, three RTD dye tests were carried out at the plant, varying level and agitation speed throughout.

For the experimental study, a pump was used to inject dye into the PS reactor, once the desired unit conditions of the polymerization CSTR were achieved. Samples were collected at predetermined intervals after the injection and analyzed for dye concentration in order to determine the RTD. The three different RTD's consisted of varying levels and agitator rpms, (65% / 120 rpm), (65% / 80 rpm), (25% / 80 rpm). Critical parameters for these studies were production rate (stable at 80 ± 5 pph) and reactor's solids (30 ± 3 %). All of this information can be found in Table 5.

Table 5. Dye Test Experimental Conditions

Experiment	RPM	Level (%)	Prod. Rate (lbs/hr)	Solids (%)
1	120	60	75	30.1
2	80	60	80	29.6
3	80	25	81	27.1

The dye target range was 0-100 ppm, with 100 ppm being the maximum instantaneous concentration of dye in the exiting stream. The method for measuring the exiting stream's concentration was color spectroscopy using a concentration curve calibrated with samples containing 0.3, 3.0, and 30 ppm blue dye in 30% converted crystal PS. The method of injection was a N_2 pressured pump filled with the necessary dye dissolved in styrene.

Results from the validation study are displayed below. Figure 10.a through Figure 10.c shows the comparison between the RTD for each experiment and the corresponding CFD prediction.

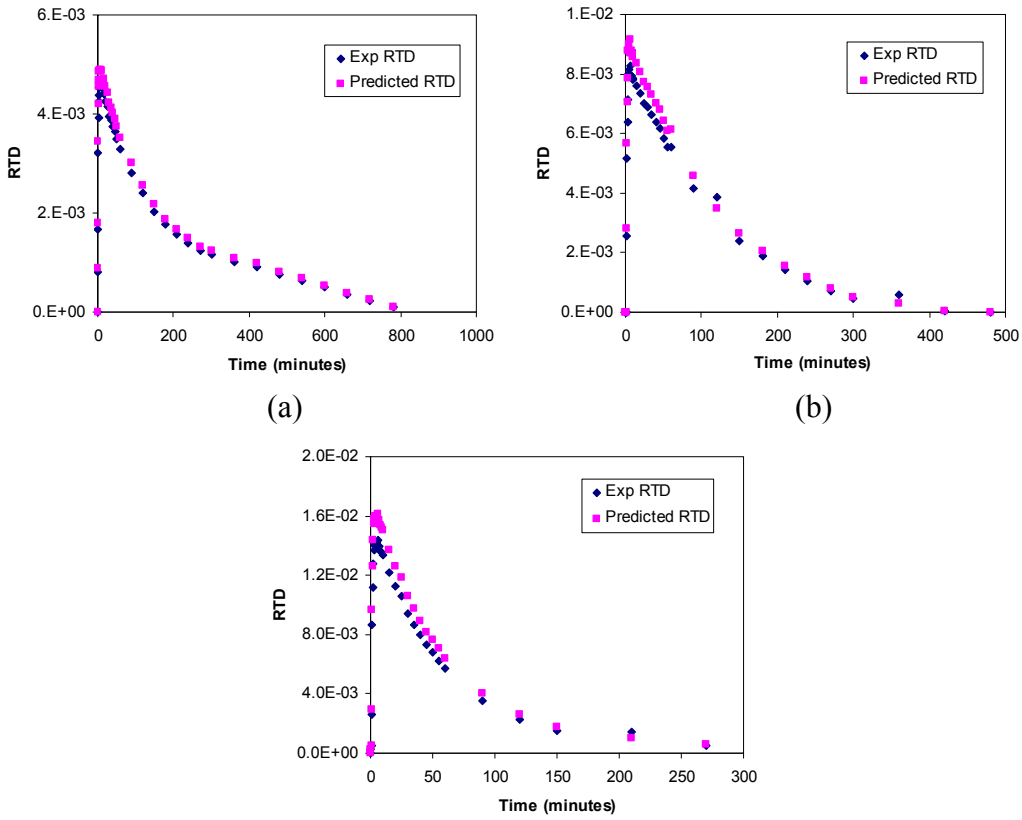

Figure 10. Comparison between RTD of Exp 1-3 and the corresponding CFD prediction

A good agreement is observed between experimental and CFD-predicted RTD. All three studies show nearly ideal CSTR behavior as indicated by the RTD graphs and the σ/t_m values (Table 6). According to the σ/t_m values, varying the agitation speed from 120 RPM to 80 RPM had some effect on the CSTR behavior with the dye exiting faster with an increased agitation speed. A decrease in level also increased the CSTR behavior, as expected.

Table 6. σ/t_m values for Exp 1 – 3

Experiment	RPM	Level	σ/t_m Exp	σ/t_m CFD
1	120	60%	0.86	0.87
2	80	60%	0.85	0.86
3	80	25%	0.92	0.94

4. MODELING OF THE CONTINUOUS POLYMERIZATION OF St

The final approach consists of two modules: the Fluid-dynamic (or RTD) Module and the Kinetic Module, based on Estenoz et al. (1996).

The first module simulates the FD of the reactor using CFD in order to obtain a 3-dimensional representation of the flow field. From the flow field, the RTD of the reactor is estimated as explained in the previous section. The second module is a 0-dimensional polymerization model and allows predicting the evolution along the residence time of global variables (such as conversion, reagent and product concentrations, and grafting efficiency), the molecular structure and the viscosity. Both modules are solved simultaneously and the variables time distributions and the corresponding average properties at the outlet stream are estimated (Figure 11).

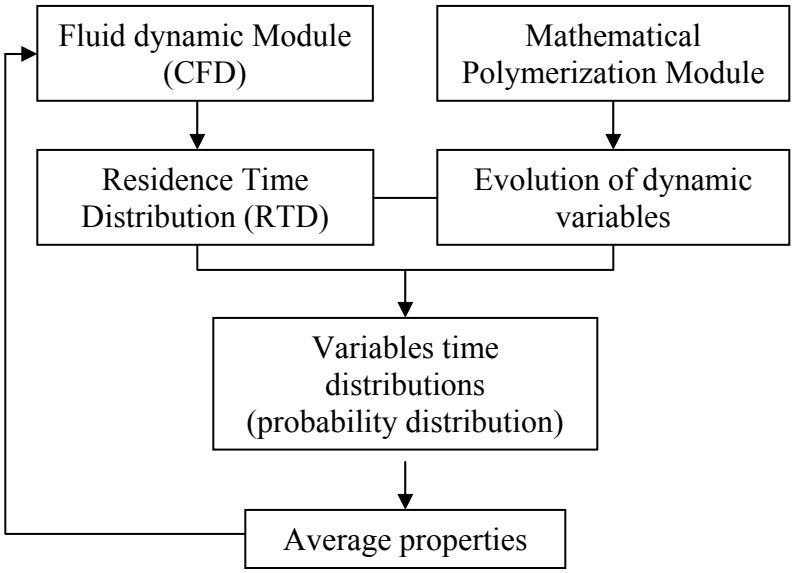

Figure 11. Iterative procedure

4.1 Kinetic Module

The kinetic module to simulate a batch operation of a stirred tank reactor is based on the kinetic mechanism of Table 7 and includes chemical and thermal initiation, propagation, transfers to the monomer, and termination by recombination.

k_d, k_i, k_{th}, k_p, k_{tm}, and k_{tc} refer to rate constants for initiator decomposition, chemical initiation, thermal decomposition, propagation, transfer to the monomer, and termination by combination, respectively.

Table 7. Kinetic mechanism

Initiator decomposition	$I_2 \xrightarrow{k_d} 2I^\bullet$
Chain initiation	$I^\bullet + St \xrightarrow{k_i} S_1^\bullet$
Thermal initiation	$3\,St \xrightarrow{k_{th}} 2S_1^\bullet$
Propagation	$S_n^\bullet + St \xrightarrow{k_p} S_{n+1}^\bullet$
Chain transfer to monomer	$S_n^\bullet + St \xrightarrow{k_{tm}} S_n + S_1^\bullet$
Termination by recombination	$S_n^\bullet + S_m^\bullet \xrightarrow{k_{tc}} S_{n+m}$

With the aim of introducing the FD in the mathematical model of a CSTR for PS production, a published kinetic model (Estenoz et al., 1996) was extended and coupled with the RTD prediction.

In Appendix B, the mathematical model for the kinetic module is presented. The final equations (B.1-B.13) allow the calculation of reagent and product concentrations, conversion, average molecular weights and viscosity. The kinetic parameters are presented in Table 8. All the expressions were directly adopted from literature.

The model consists of a system of differential-algebraic equations that is solved by standard numerical methods, appropriate for "stiff" differential equations. The computer program was written in Octave. A typical simulation consumed about 10 seconds to solve the polymerization module.

Table 8. Kinetic parameters

f		0.57	Gonzalez et al., 1996
k_d	[1/s]	$9.13\times10^{13}\,e^{-29{,}508/RT}$	Gonzalez et al., 1996
k_{th}	[L^2/(mol^2.s)]	$2.10\times10^{6}\,e^{-15{,}000/T}$	Peng, 1990
k_i	[L/(mol.s)]	$8.37\times10^{5}\,e^{-2{,}650/T}$	Estenoz et al., 1996
k_p	[L/(mol.s)]	$9.56\times10^{5}\,e^{-2{,}600/T}$	Villalobos et al.,1991
k_{tm}	[L/(mol.s)]	$7.81\times10^{6}\,e^{-6{,}435/T}$	Brandrup et al., 1989
k_{tc}	[L/(mol.s)]	$1.66\times10^{9}\,e^{-(843/T)-2(A_1x+A_2x^2+A_3x^3)}$	Hamielec et al., 1976

$A_1 = 2.57 - 0.00505T$; $A_2 = 9.56 - 0.0176T$; $A_3 = -3.03 + 0.00785T$

4.2. Coupling of polymerization module with the RTD prediction

Considering that the kinetic is not affected by the shear rate and the flow field (no degradation reactions occur), and evaluating the effect of the polymerization degree on the FD through the average properties, an iterative procedure was applied in order to couple the polymerization and FD modules.

The kinetic model simulates the evolution of the dynamic variables (conversion, viscosity, molecular weight) along each residence time. Considering the results predicted by the polymerization model and the RTD from the CFD calculation, a probability distribution of the chemical magnitudes at the outlet of a CSTR can be obtained.

Using statistical calculation, average properties can be calculated from these distributions. Then, the flow field is recalculated with the CFD model using the predicted average properties. This iterative procedure is applied until convergence of the average variables.

To check the iterative algorithm, the geometry of the reactor considered in Ring et al. (2004) was simulated. For the kinetic module resolution, a bulk polymerization of St in the presence of 1 ppm of BPO initiator was considered. The simulation was carried out at 90ºC with a flow rate 40 ml/min.

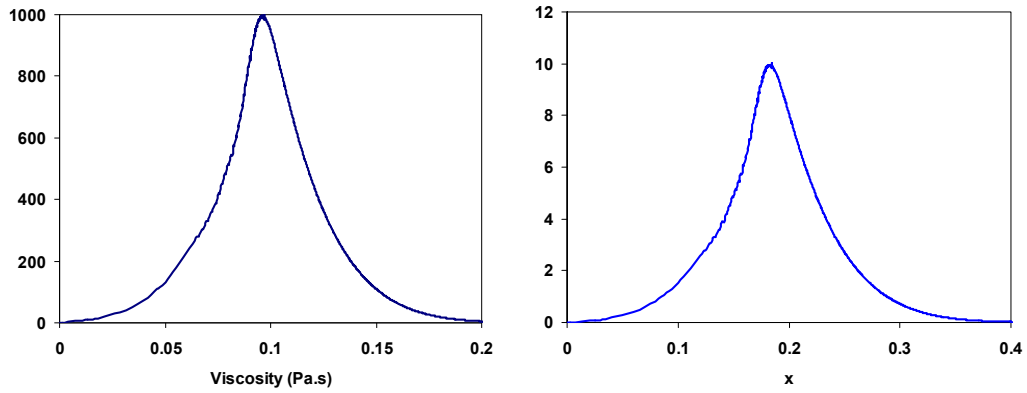

(a) (b)

Figure 12. Predicted variables distributions: a) viscosity; b) conversion

Based on the value of the Reynolds number, a laminar regime was found in the course of the simulation.

The number of iterations to achieve the convergence between the polymerization and FD modules was less than 10.

In Figure 12, distributions of the viscosity and conversion predicted by the model are represented. A final average viscosity of 0.1 Pa.s and a 20% average monomer conversion were predicted.

In Table 9, the results predicted by kinetic-CFD model are compared with the corresponding values obtained assuming an ideal CSTR. The same kinetic constants are used in both simulations. It can be noted that if the molecular weights are compared, they differ from each other due to the non-ideal deviation of the system (an increase in the mean RT due to the presence of dead zones). As expected, a broader polydispersity (D_p) was obtained for the non-ideal system.

Table 9. Comparison between predicted results for an ideal and non-ideal reactor during the polymerization of St

Tank space-time V_R/Q (min)	t_m (min)		$\overline{M}_n$		$\overline{M}_w$		D_p	
	ideal	non-ideal	ideal	non-ideal	ideal	non-ideal	ideal	non-ideal
100	100	107	118,800	128,700	241,100	293,400	2.03	2.28

5. CONCLUSIONS

The interaction between the polymerization model and CFD studies will lead us to obtain recipes and reaction conditions for the production of a priori specified grades of PS.

The prediction of a complete velocity distribution in a CSTR and the determination of its RTD were carried out with the aid of the commercial CFD software Fluent 6.3. The stimulus-response tracer method showed a good performance and it was reasonably accurate for obtaining a complete RTD compared to the particle tracking method. CFD results were validated with different experimental data and very good agreements were obtained in all cases.

A new approach to simulate the continuous operation of a stirred tank reactor for St polymerization was proposed. A kinetic model for the batch operation of a stirred tank reactor was coupled with RTD predictions (CFD) in order to calculate the probability distributions of the chemical magnitudes at the outlet and the average properties. An iterative procedure was applied and the convergence was tested.

For the cases studied, the results predicted by the CFD-kinetic model were close to the corresponding values obtained by an ideal CSTR model. The predicted molecular weights were very similar, but a lower D_p in the ideal model was obtained. However, this approach can be useful when simulating other reaction conditions including industrial process where an important effect of the FD on the final polymer quality is expected.

In a future work, the polymerization module will be incorporated into the CFD model and the variation of viscosity, composition, density and molecular weight in the course of the reaction will be included in the continuity, momentum, energy, and species transport equations. To this effect, the polymerization reaction kinetics will be incorporated by standard user-defined functions (UDFs) coded in C language. The UDF code will be written for the reaction source terms linked to the species transport model coded in Fluent. The approach consists of solving conservation equations for chemical species. The model will predict the local mass fraction of each species by means of the resolution of a convection-diffusion equation for every species. The advantage of this coupling method is that the model can simultaneously solve the fluid dynamics and kinetics iterating between them in every cell.

Other "engineering" application of the mathematical model is the design of operation strategies in order to produce PS with "a priori" specified characteristics. To this effect, the use of appropriate optimization routines or other computational techniques (such as neural network, genetic algorithms, particle swarm optimization) in combination with the reactor model can be evaluated.

APPENDIX A

Fluid-dynamic Module

The hydrodynamic module consists of the Continuity and Momentum equations.

Continuity Equation

$$\frac{\partial}{\partial x_i}(\rho u_i) = 0 \tag{A.1}$$

where ρ is the density and u_i is the velocity in the direction i.

Momentum Equation

For a laminar regime, the momentum balance (or Navier-Stokes equation) can be written for each coordinate component as follows:

$$\frac{\partial}{\partial x_j}(\rho u_i u_j) = -\frac{\partial p}{\partial x_i} + \frac{\partial}{\partial x_j}\left[\mu\left(\frac{\partial u_i}{\partial x_j} + \frac{\partial u_j}{\partial x_i} - \frac{2}{3}\frac{\partial u_k}{\partial x_k}\delta_{ij}\right)\right] + \rho g_i + F_i \tag{A.2}$$

where the convection terms are on the left hand side and the terms on the right hand side are the pressure gradient, the diffusion of momentum, the gravitational force, and other generalized forces (source terms), respectively.

In the turbulent regime, the momentum balance can be written on the basis of the average velocities $\bar{u}_i$ and the fluctuating components $\bar{u}'_i$ following the Reynolds-Averaged Navier-Stokes or RANS equation for momentum:

$$\frac{\partial}{\partial x_j}(\rho \bar{u}_i \bar{u}_j) = -\frac{\partial \bar{p}}{\partial x_i} + \frac{\partial}{\partial x_j}\left[\mu\left(\frac{\partial \bar{u}_i}{\partial x_j} + \frac{\partial \bar{u}_j}{\partial x_i} - \frac{2}{3}\frac{\partial \bar{u}_k}{\partial x_k}\delta_{ij}\right)\right] + \frac{\partial}{\partial x_j}(-\rho\overline{u'_i u'_j}) + \rho g_i + F_i \tag{A.3}$$

The term involving $\overline{u'_i u'_j}$ is the Reynolds stress term.

Introducing the Boussinesq hypothesis, the Reynolds stress can be expressed in terms of mean velocity gradients, as follows:

$$\rho\overline{u'_i u'_j} = \frac{2}{3}\rho k \delta_{ij} + \left[\mu_t\left(\frac{\partial u_i}{\partial x_j} + \frac{\partial u_j}{\partial x_i}\right)\right] \tag{A.4}$$

where μ_t is the turbulent viscosity; and k is the kinetic energy of turbulence defined in terms of the velocity fluctuations u', v', and w' in each of the three coordinate directions:

$$k = \frac{1}{2}\left(\overline{u'^2} + \overline{v'^2} + \overline{w'^2}\right) \tag{A.5}$$

Including the standard k-ε turbulent model in the N-S equations, it results:

$$\frac{\partial}{\partial x_i}(\rho u_i k) = \frac{\partial}{\partial x_i}\left(\mu + \frac{\mu_t}{\sigma_k}\right)\frac{\partial k}{\partial x_i} + G_k - \rho\varepsilon \tag{A.6}$$

$$\frac{\partial}{\partial x_i}(\rho u_i \varepsilon) = \frac{\partial}{\partial x_i}\left(\mu + \frac{\mu_t}{\sigma_\varepsilon}\right)\frac{\partial \varepsilon}{\partial x_i} + C_1\frac{\varepsilon}{k}G_k + C_2\rho\frac{\varepsilon^2}{k} \tag{A.7}$$

where ε is the rate of turbulence dissipation; C_1, C_2, σ_k, and σ_ε are empirical constants; and G_k is a generation term for turbulence that can be calculated from:

$$G_k = \mu_t \left(\frac{\partial u_i}{\partial x_j} + \frac{\partial u_j}{\partial x_i} \right) \frac{\partial u_j}{\partial x_i} \tag{A.8}$$

The turbulent viscosity μ_t is derived from both k and ε, and involves a constant taken from experimental data, C_μ, which has a value of 0.09 (Deglon et al., 2006):

$$\mu_t = \rho C_\mu \frac{k^2}{\varepsilon} \tag{A.9}$$

APPENDIX B

Kinetic module

The polymerization module consists of the material balances that follow, derived from the global mechanism of Table 7.

Applying the mass balance equation for the elementary species of the reaction mixture, an infinite set of differential equations is obtained, representing the first form of the kinetic model of the considered system.

The method of moments has been applied in order to reduce and convert the thousands of polymerization steps into a conventional reaction scheme that has a manageable size, and to compute the product characteristics, such as molecular weight distribution (MWD) and polydispersity. In this method, the moments of live radical and dead polymer chain are defined as:

$$\begin{aligned} [\lambda_0] &= \sum_{n=1}^{\infty} [S_n^\bullet] \qquad [\lambda_1] = \sum_{n=1}^{\infty} n [S_n^\bullet] \qquad [\lambda_2] = \sum_{n=1}^{\infty} n^2 [S_n^\bullet] \\ [\mu_0] &= \sum_{n=1}^{\infty} [S_n] \qquad [\mu_1] = \sum_{n=1}^{\infty} n [S_n] \qquad [\mu_2] = \sum_{n=1}^{\infty} n^2 [S_n] \end{aligned} \tag{B.1}$$

where n is the number of radicals or polymer chains or the degree of polymerization, λ_i represents the moments of the radicals, and μ_i represents the moments of the polymers. By doing the corresponding calculations over the total range of variation of n, the following set of species source terms can be derived:

Initiator

$$\frac{1}{V} \frac{d}{dt} ([I_2] V) = -k_d [I_2] \tag{B.2}$$

Monomer

Assuming the "long chain approximation" (by which propagation is the only monomer-consuming reaction), one can write:

$$\frac{1}{V}\frac{d}{dt}([St]V) = -k_p[St][\lambda_0] = -R_p \tag{B.3}$$

where R_p is the global rate of St consumption and $[\lambda_0]$ is the total concentration of $S^{\bullet}_n$ radicals.

Radical Species

$$\frac{1}{V}\frac{d}{dt}([I^{\bullet}]V) = 2fk_d[I_2] - k_i[I^{\bullet}][St] \tag{B.4}$$

where f is the initiator efficiency. It stands for the fraction of the initiator amount that participates in the reaction.

The quasi-state state approximation (QSSA) is applied. The QSSA assumes that the effective rate of the increasing radical chain formation is close to zero.

$$\frac{1}{V}\frac{d}{dt}([I^{\bullet}]V) = 0 \Rightarrow [I^{\bullet}] = \frac{2fk_d[I_2]}{k_i[St]} \tag{B.5}$$

$$\frac{1}{V}\frac{d}{dt}([\lambda_0]V) = 2fk_d[I_2] + 2k_{th}[St]^3 - k_{tc}[\lambda_0]^2 \tag{B.6}$$

$$\begin{aligned}\frac{1}{V}\frac{d}{dt}([\lambda_1]V) = {} & 2fk_d[I] + 3k_{th}[St]^3 + k_p[St][\lambda_0] \\ & - k_{tm}[St]([\lambda_1] - [\lambda_0]) - k_{tc}[\lambda_0][\lambda_1]\end{aligned} \tag{B.7}$$

$$\begin{aligned}\frac{1}{V}\frac{d}{dt}([\lambda_2]V) = {} & 2fk_d[I] + 5k_{th}[St]^3 + k_p[St](2[\lambda_1] + [\lambda_0]) \\ & - k_{tm}[St]([\lambda_2] - [\lambda_0]) - k_{tc}[\lambda_0][\lambda_2]\end{aligned} \tag{B.6}$$

$$\frac{1}{V}\frac{d}{dt}([\mu_0]V) = k_{tm}[St][\lambda_0] + 1/2k_{tc}[\lambda_0]^2 \tag{B.7}$$

$$\frac{1}{V}\frac{d}{dt}([\mu_1]V) = k_{tm}[St][\lambda_1] + k_{tc}[\lambda_0][\lambda_1] \tag{B.8}$$

$$\frac{1}{V}\frac{d}{dt}([\mu_2]V) = k_{tm}[St][\lambda_2] + k_{tc}\left([\lambda_1]^2 + [\lambda_0][\lambda_2]\right) \tag{B.9}$$

Molecular Weight Distribution

The moments can also be used to obtain the number-average and mass-average molecular weights:

$$\overline{M}_n = M_M \frac{\mu_1}{\mu_0} \tag{B.10}$$

$$\overline{M}_w = M_M \frac{\mu_2}{\mu_1} \tag{B.11}$$

where MW_M is the molecular weight of monomer. The polydispersity, D_p, a measure of relative dispersion of the molecular weight distribution, is defined as:

$$D_p = \frac{\mu_0 \mu_2}{{\mu_1}^2} \tag{B.12}$$

Viscosity

The viscosity is calculated with the correlation found in Kim and Nauman (1992) for St polymerization.

$$\begin{aligned} \ln \mu = -11.091 + \frac{1109}{T} + M_{PS}^{0.1413}\Big[12.032 w_{PS} - 19.501 w_{PS}^2 + 2.923 w_{PS}^3 \\ + \left(-1327 w_{PS} + 1359 w_{PS}^2 + 3597 w_{PS}^3\right)/T\Big] \end{aligned} \tag{B.13}$$

where M_{PS} is the PS molecular weight and w_{PS} is the mass fraction of PS.

REFERENCES

Atiemo-Obeng V.A., Paul E.L. and Kresta S.M., "Handbook of Industrial Mixing: Science and Practice", Wiley-IEEE, 2004.

Bakker A, Haidari A H. and Marshall L. M., "Design Reactors via CFD", Chemical Engineering Progress, 2001, 97, 12, 31-39.

Brandrup J. and Immergut E. H., Polymer Handbook, 3rd ed., Wiley, New York, 1989.

Brooks B. W., "Why Polymerization Reactors are Special?" Industrial & Engineering Chemical Research, 1997, 36, 4, 1158-1162.

Cole W. M., "Experimental Study of Mixing Patterns in Continuous Polymerization Reactors and their Effect on Polymer Structure", AIChE Symposium Series, 1975, 72, 160, 51.

Dhib R., Patel H. and Ein-Mozaffari F., "CFD Analysis of Mixing in Thermal Polymerization of Styrene", Computers and Chemical Engineering, 2010, 34, 421–429.

Ein-Mozaffari F., Patel H. and Dhib R., "Computational Fluid Dynamics Study of a Styrene Polymerization Reactor", Chemical Engineering & Technology, 2010, 33, 2, 258-266.

Estenoz D. A., Valdez E., Oliva H. M. and Meira G. R., "Bulk Polymerization of Styrene in Presence of Polybutadiene: Calculation of Molecular Macrostructure", Journal of Applied Polymer Science, 1996a, 59, 861.

Ghirelli F., Hermansson S., Thunman H. and Leckner B., "Reactor Residence Time Analysis with CFD", Prog. Computational Fluid Dynamics: International Journal (PCFD), 2006, 6(4/5).

González I.M., Meira G.R., and Oliva H., "Synthesis of Polystyrene with Mixtures of Mono- and Bifunctional Initiators", Journal of Applied Polymer Science, 1996, 59, 6, 1015-1026.

Hamielec A. E. and Friis N., "Gel-Effect in Emulsion Polymerization of Vinyl Monomers", ACS Symposium Series, 1976, 24, 82.

Harada M., Tanaka K., Eguchi W. and Nagata, S., "The Effect of Micro-Mixing on the Homogeneous Polymerization of Styrene in a Continuous Flow Reactor", Journal of Chemical Engineering of Japan, 1968, 1, 2, 148.

Harshe Y.M., Utikar R.P. and Ranade V.V., "A Computational Model for Predicting Particle Size Distribution and Performance of Fluidized Bed Polypropylene Reactor", Chemical Engineering Science, 2004, 59, 5145-5156.

Hatzantonis H., Yiannoulakis H., Yiagopoulos A. and Kiparissides C., "Recent Developments in Modeling Gas-Phase Catalyzed Olefin Polymerization Fluidized-Bed Reactors: The Effect of Bubble Size Variation on the Reactor's Performance", Chemical Engineering Science, 2000, 55, 16, 3237-3259.

Hayes R.E., "Introduction to Chemical Reactor Analysis", Taylor & Francis, New York, 2001.

Heidarian J., Nayef M. G. And Wan M. A. W., "Effects of the Temperature and Mixing Rate on Foaming in a Polymerization Reaction to Produce Fatty Polyamides in the Presence of Catalyst", Industrial & Engineering Chemistry Research, 2004, 43, 19, 6048.

Kemmere M. F., Meuldljk J., Drinkenburg A. A. H. and German A. L., "Emulsification in Batch-Emulsion Polymerization of Styrene and Vinyl Acetate: A Reaction Calorimetric Study", Journal of Applied Polymer Science, 2001, 79, 5, 944.

Kim D. and Nauman E., "Solution Viscosity of Polystyrene at Conditions Applicable to Commercial Manufacturing Processes", Journal of Chemical & Engineering Data, 1992, 37, 427-432.

Kim J.Y. and Laurence R.L., "The Mixing Effect on the Free Radical MMA Solution Polymerization", Korean Journal of Chemical Engineering, 1998, 15, 3, 273.

Kolhapure N. H. and Fox R. O., "CFD Analysis of Micro Mixing Effects on Polymerization in Tubular Low Density Polyethylene Reactors", Chemical Engineering Science, 1999, 54, 15, 3233-3242.

Levenspiel O., Lai B.W. and Chatlynne C.Y., "Tracer Curves and the Residence Time Distribution", Chemical Engineering Science, 1970, 25, 1611–1613.

Levenspiel O., "Chemical Reaction Engineering" (Third edition), John Wiley & Sons, USA, 1999.

Li K.T. and Lee J.D., "Mixing and Control of a CSTR with Series-Parallel Reactions", Journal Chinese Institute of Chemical Engineers, 1991, 22, 2, 61–69.

Mahling F. O., Daib A., Kolhapure N. and Fox R. O., "CFD Analysis of Heat Transfer and Initiator Mixing Performance in LDPE High Pressure Tubular Reactors", European Symposium on Computer Aided Process Engineering, 2000, 427-432.

Meszena Z. G. and Johnson A. F., "Prediction of the Spatial Distribution of the Average Molecular Weights in Living Polymerization Reactors using CFD Methods", Macromolecular Theory and Simulation, 2001, 10, 2, 123-135.

Newell B., Bailey J., Islam A., Hopkins L. and Lant P., "Characterizing Bioreactor Mixing with Residence Time Distribution Tests", Water Science Technology, 1998, 37, 12, 43–47.

Prochukhan Y. A., Minsker K. S., Karpasas B. A., Bakhitova R. K. and Yenikolopyan N. S., "Effect of Mixing Methods on the Character of Ultra-Fast Polymerization Processes", Polymer Science, 1988, 30, 6, 1317.

Ranade V., "Computational Flow Modeling for Chemical Reactor Engineering", Academic Press, New York, 2002.

Read K., Zhang X. and Ray W. H., "Simulation of a LDPE Reactor Using Computational Fluid Dynamics", AIChE Journal, 1997, 1, 43, 104.

Ring T.A, Choi B.S., Wan B., Philyaw S. and Dhanasekharan K., "Residence Time Distributions in a Stirred Tank: Comparison of CFD Predictions with Experiment", Industrial & Engineering Chemistry Research, 2004, 43, 20, 6548–6556.

Saeed S. and Ein-Mozaffari F., "Using Dynamic Tests to Study the Continuous Mixing of Xanthan Gum Solutions", Journal of Chemical Technology and Biotechnology, 2008, 83, 4, 559-568.

Saeed S., Ein-Mozaffari F., and Upreti S.R., "Using Computational Fluid Dynamics to Study the Dynamic Behavior of the Continuous Mixing of Herschel-Bulkley Fluids", 2008, 47, 19, 7465-7475.

Soliman M. A., Aljarboa T. and Alahmad M., "Simulation of Free Radical Polymerization Reactors", Polymer Engineering & Science, 1994, 19, 34, 1464-1470.

Thyn J., Ha J.J., Strasak P. and Zitny R., "RTD Prediction, Modeling and Measurement of Gas Flow in Reactor", Nukleonika, 1998, 43, 1, 95–114.

Tosun G., "A Mathematical Model of Mixing and Polymerization in a Semi Batch Stirred Tank Reactor", AIChE Journal, 1992, 38, 425.

Tosun G. and Bakker A., "A Study of Macro-Segregation in Low-Density Polyethylene Autoclave Reactors by Computational Fluid Dynamics Modelling", Industrial & Engineering Chemistry Research, 1997, 36, 2, 296-305.

Turley S. G. and Keskkula H., "Effect of Rubber-Phase Volume Fraction in Impact Polystyrene on Mechanical Behavior", Polymer, 1980, 21, 466.

Turner J.C.R., "The Interpretation of Residence Time Measurements in Systems with and without Mixing", Chemical Engineering Science, 1971, 26, 549–557.

Vedantam S. and Joshi J.B., "CFD Simulation of RTD and Mixing in the Annular Region of a Taylor-Couette Contactor", Industrial & Engineering Chemistry Research, 2006, 45, 18, 6360–6367.

Verazaluce J., Flores A. and Saldivar E., "Steady-state Nonlinear Bifurcation Analysis of a High-Impact Polystyrene Continuous Stirred Tank Reactor", Industrial & Engineering Chemistry Research, 2000, 39, 6, 1972-1979.

Villa C. M., Dihora J. O. and Ray W. H., "Effects of Imperfect Mixing on Low-Density Polyethylene Reactor Dynamics", AIChE Journal, 1998, 44, 7, 1646.

Villalobos M. A, Hamielec A. E. And Wood P. E., "Kinetic Model for Short-Cycle Bulk Styrene Polymerization through Bifunctional Initiators", Journal of Applied Polymer Science, 1991, 42, 629.

Wells G. J. and Ray W. H., "Investigation of Imperfect Mixing Effects in the LDPE Autoclave Reactor using CFD and Compartment Models", DECHEMA Monographs, 2001, 137, 49-59.

Yiannoulakis H., Yiagopoulos A. and Kiparissides C., "Recent Developments in the Particle Size Distribution Modeling of Fluidized-Bed Olefin Polymerization Reactors" Chemical Engineering Science, 2001, 56, 3, 917-925.

Zaloudik P., "Mixed Model for Continuous Stirred Tank Reactor with Viscous Fluid from Experimental Age Distribution Study", 1969, Reaction Engineering, 14, 5, 657–659.

Zhou W., Marshall E. and Oshinowo L., "Modelling LDPE Tubular and Autoclave Reactor", Industrial & Engineering Chemistry Research, 2001, 40, 23, 5533-5542.